Acta Oceanol. Sin., 2020, Vol. 39, No. 12, P. 106–113
https://doi.org/10.1007/s13131-020-1641-x
http://www.hyxb.org.cn
E-mail: hyxbe@263.net

Noise reduction of acoustic Doppler velocimeter data based on Kalman filtering and autoregressive moving average models

Chuanjiang Huang[1, 2, 3], Fangli Qiao[1, 2, 3*], Hongyu Ma[1, 3]

[1] First Institute of Oceanography, Ministry of Natural Resources, Qingdao 266061, China

[2] Laboratory for Regional Oceanography and Numerical Modeling, Pilot National Laboratory for Marine Science and Technology (Qingdao), Qingdao 266237, China

[3] Key Laboratory of Marine Sciences and Numerical Modeling, Ministry of Natural Resources, Qingdao 266061, China

Received 27 February 2020; accepted 30 May 2020

Abstract

Oceanic turbulence measurements made by an acoustic Doppler velocimeter (ADV) suffer from noise that potentially affects the estimates of turbulence statistics. This study examines the abilities of Kalman filtering and autoregressive moving average models to eliminate noise in ADV velocity datasets of laboratory experiments and offshore observations. Results show that the two methods have similar performance in ADV de-noising, and both effectively reduce noise in ADV velocities, even in cases of high noise. They eliminate the noise floor at high frequencies of the velocity spectra, leading to a longer range that effectively fits the Kolmogorov –5/3 slope at mid-range frequencies. After de-noising adopting the two methods, the values of the mean velocity are almost unchanged, while the root-mean-square horizontal velocities and thus turbulent kinetic energy decrease appreciably in these experiments. The Reynolds stress is also affected by high noise levels, and de-noising thus reduces uncertainties in estimating the Reynolds stress.

Key words: noise, Kalman filtering, autoregressive moving average model, turbulence, acoustic Doppler velocimeter

Citation: Huang Chuanjiang, Qiao Fangli, Ma Hongyu. 2020. Noise reduction of acoustic Doppler velocimeter data based on Kalman filtering and autoregressive moving average models. Acta Oceanologica Sinica, 39(12): 106–113, doi: 10.1007/s13131-020-1641-x

1 Introduction

The acoustic Doppler velocimeter (ADV) can effectively measure three-dimensional instantaneous velocities at relatively high sampling rates. It has been widely used for estimates of turbulence characteristics in hydrologic and hydraulic measurements (Chang et al., 2019; Qi et al., 2020). However, turbulence measurements made by the ADV suffer from random spikes (Goring and Nikora, 2002) and noise (Voulgaris and Trowbridge, 1998; Nikora and Goring, 1998). Adequate post-processing, including de-spiking and de-noising, is necessary to obtain reliable turbulence parameters.

The spikes in ADV datasets are mainly induced by aliasing of the Doppler signal (McLelland and Nicholas, 2000). A number of methods of de-spiking have been proposed (Goring and Nikora, 2002; Wahl, 2003; Mori et al., 2007; Parsheh et al., 2010; Islam and Zhu, 2013; Dilling and MacVicar, 2017), and can eliminate spurious outliers and spikes in ADV time series. There are three categories of noise in ADV measurements, among which Doppler noise is the most notable and inherent to the measuring principle of the ADV (Voulgaris and Trowbridge, 1998). Doppler noise is proportional to the velocity range setting and the square root of the sampling frequency (SonTek, 2001). It also depends on the flow characteristics and the type of particles in the water (Nikora and Goring, 1998; Lemmin and Lhermitte, 1999).

The velocity range determines the maximal velocity that can be measured by the ADV. In oceanic observations, a large velocity range is typically selected to account for tide currents and the orbital velocity of surface waves (Elgar et al., 2005; Feddersen, 2010). Moreover, turbulent measurements require high sampling frequencies to avoid the loss of high-frequency turbulence information (García et al., 2005). However, a large velocity range and a high sampling frequency usually result in a high noise energy level in the signal. Thus, measurements of turbulence made in the ocean using an ADV always have high noise energy levels. Meanwhile, the noise level in the ADV horizontal velocity components is much larger than that in the vertical component, owing to the geometric structure of the sensor. The ratio of these noise levels can exceed 30 in practical observations (Voulgaris and Trowbridge, 1998; Wolk et al., 2002).

Doppler noise in ADV velocities is considered to be Gaussian white noise approximately (Nikora and Goring, 1998), and thus it does not affect the mean value of velocity. However, this noise potentially affects the statistical characteristics of turbulence (Goring and Nikora, 2002; Khorsandi et al., 2012), especially those associated with horizontal velocity components. This usually leads to overestimation of the horizontal root-mean-square (RMS) velocities and thus turbulent kinetic energy. The overestimation of the horizontal RMS velocities can affect the applicab-

Foundation item: The National Key Research and Development Program of China under contract No. 2017YFC1404000; the Basic Scientific Fund for National Public Research Institutes of China under contract No. 2018S03; the National Natural Science Foundation of China under contract Nos 41776038 and 41821004.

*Corresponding author, E-mail: qiaofl@fio.org.cn

ility evaluation of Taylor's frozen turbulence hypothesis (Sadoughi and Veeravalli, 1994; Bluteau et al., 2011), which is a prerequisite for the transformation of spectra between temporal and spatial domains.

Hurther and Lemmin (2001) estimated the noise contribution to turbulence parameters using two independent but simultaneously measured vertical velocities. This method is only valid for four-receiver ADV instruments and not typical ADVs with three receivers. Durgesh et al. (2014) proposed two different approaches, the noise auto-correlation and proper orthogonal decomposition, to reduce the level of noise in ADV velocity spectra. As they pointed out, the first approach does not provide noise-corrected data in the temporal domain; the other approach is more computationally intensive and requires a prior estimate of the noise level or spectral shape. Qiao et al. (2016) and Huang et al. (2018) adopted empirical mode decomposition to eliminate Doppler noise. However, this method tends to eliminate all the energy of selected modes and it is thus applied usually to ADV datasets with a low noise level.

In this paper, we examine the abilities of Kalman filtering (KF) and autoregressive moving average (ARMA) models to remove noise from ADV datasets by conducting laboratory experiments and offshore observations. These two methods are briefly introduced in Section 2. Results are presented in Section 3 for laboratory experiments and Section 4 for offshore observations. Section 5 presents conclusions drawn from the results of the paper.

2 Methods and data processing

2.1 *Kalman filtering*

KF is an efficient recursive filter proposed by Kalman (1960) for time-varying linear systems and is widely used in the time-series analysis of dynamic data. This filter incorporates past measurement estimation errors into new measurement errors to estimate future errors. It minimizes the mean-square prediction error and can eliminate random interference error contained in the data (i.e., noise pollution), to provide an optimal estimation of the real observation.

The evolution of a state variable x in time is described by the system equation:

$$x_{k+1} = A_k x_k + \eta_k, \tag{1}$$

and is associated with observations z_k according to

$$z_k = H_k x_k + \varepsilon_k, \tag{2}$$

where the matrices A_k and H_k are respectively the system and observation operators. The random variables η and ε are respectively noise in the system and noise in the observation evolution, and are assumed to be white Gaussian noise with covariances Q and R, respectively.

At time k, the best estimate of x_k is $\widehat{x}_k$ and its covariance matrix is P_k. From time step k to k+1, they are calculated as

$$\widehat{x}_{k+1}^{-} = A_k \widehat{x}_k, \tag{3}$$

$$P_{k+1}^{-} = A_k P_k A_k^T + Q_k. \tag{4}$$

The superscript "–" represents the a priori state estimate. In the measurement update that follows, the Kalman gain is firstly estimated as

$$K_k = P_k^{-} H_k^T (H_k P_k^{-} H_k^T + R_k)^{-1}. \tag{5}$$

The next step is to calculate the actual observation z_k:

$$\widehat{x}_k = \widehat{x}_k^{-} + K_k \left(z_k - H_k \widehat{x}_k^{-}\right), \tag{6}$$

$$P_k = (I - K_k H_k) P_k^{-}. \tag{7}$$

The filtering process is to estimate the value of the observation time according to the estimation of the previous time, then to revise the estimation according to the observation value, and finally to get the optimal estimation of the observation time, so as to achieve the effect of filtering. This method was described in detail by Welch and Bishop (1995).

A standard KF program obtained from a publicly accessible package provided by Moore (2012) was used in the present study. In this program, only a few parameters need to be specified by the user. In the following study, the exponentially weighted moving average was used to estimate time-varying system covariances, in which the lengths of the moving average and lookback window were empirically set to 48 and 24 for the horizontal velocity components, and 12 and 6 for the vertical component, respectively.

2.2 *Autoregressive moving average model*

Each stationary process can be effectively approximated by adopting an ARMA process, and the ARMA model is then applied extensively to time-series analysis for stationary processes (Neusser, 2016). Dilling and MacVicar (2017) used this method to detect and replace spikes in ADV datasets. ARMA comprises two parts, an autoregressive (AR) part and a moving average (MA) part, and can be expressed as

$$u_t = -\sum_{i=1}^{p} a_i u_{t-i} + \sum_{j=0}^{q} b_j \varepsilon_{t-j}, \tag{8}$$

where u_t is the time series, p is the order of the AR term, q is the order of the MA term, a_i is the AR coefficient, b_j is the MA coefficient, and ε_{t-j} is white noise.

This model first tests the series for stationarity and identifies the appropriate orders of AR and MA terms. Once an appropriate lag order is identified, it is then determined whether the model is adequate. If the model is adequate, the residuals (ε_t) of the model are expected to be white noise (Fabozzi et al., 2014). In this study, ARMA was performed using the function ARMAX in Matlab software.

2.3 *Data processing*

The raw datasets measured by the ADV must be appropriately preprocessed before conducting statistical analyses (Chanson et al., 2007). In this paper, the preprocessing of the ADV datasets includeds three steps: de-spiking, de-noising, and coordinate rotation. First, the true three-dimensional phase space method of Mori et al. (2007) was used to remove spikes from the raw ADV time series. Second, KF or ARMA was used to reduce the level of noise. Last, double rotation was applied to rotate three-dimensional velocities into an along-stream component u, a

cross-stream component v, and a vertical component w, and the mean velocity and other turbulence parameters were then calculated.

3 Laboratory experiments

Four experiments were conducted in a channel flume under conditions of uniform flow. This flume was 32.5 m long, 1.0 m wide, and 1.8 m high and had a water depth of 1.2 m. These four experiments, referred to as Exps A1, A2, A3, and A4, had mean current speeds of 5.6 cm/s, 11.8 cm/s, 18.1 cm/s, and 24.3 cm/s, respectively. A Nortek ADV with an acoustic frequency of 6 MHz was used to measure the instantaneous three-dimensional velocity. The sampling frequency was set at 64 Hz, and a total of 19 200 data points were thus recorded for a sampling length of 5 min in each experiment.

The time series of velocities measured in Exp A2 are shown in Fig. 1 while the velocity spectra are shown in Fig. 2. Previous studies found that the horizontal velocity components of the ADV (i.e., u and v) have approximately the same noise energy level (Nikora and Goring, 1998), and only u is analyzed in the following sections. In the present study, the spectra were calculated using Welch's method, whereby the total dataset was divided into eight segments with 50% overlap and tapered with a Hamming window. A fast Fourier transform of 4 096 points was used in the spectrum density estimate.

According to Kolmogorov's theory of turbulence (Pope, 2000), the clean power spectrum of turbulence has a low-frequency energy-containing subrange, followed by an inertial subrange characterized by a –5/3 slope in log-log space, and a high-frequency viscous subrange where the decay is more rapid than that of the –5/3 slope. The spectra of only de-spiked velocities in Exp A2 are in good agreement with the –5/3 curve at mid-range frequencies

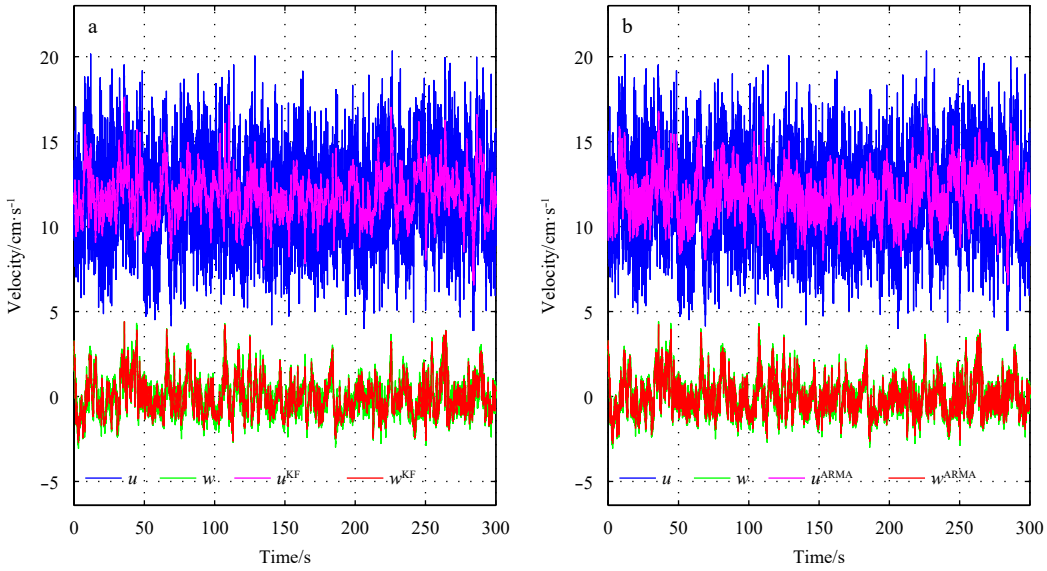

Fig. 1. Time series of de-spiked and de-noised velocities in Exp A2: KF (a) and ARMA (b). Blue and green curves are de-spiked along-stream and vertical ADV velocities, while pink and red curves are respectively those further de-noised.

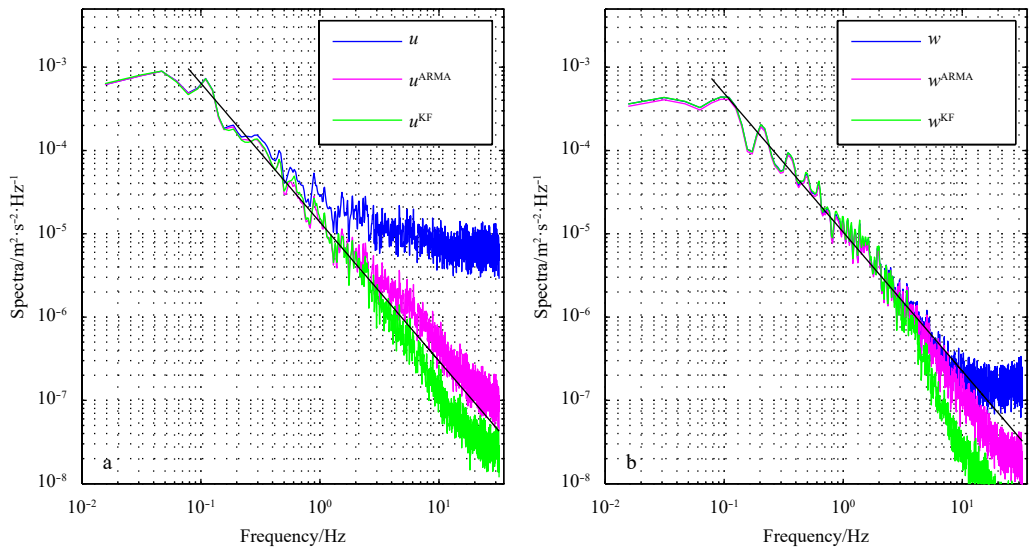

Fig. 2. Power spectra of along-stream (a) and vertical velocities (b) in Exp A2. Blue curves are the power spectra of de-spiked velocities while green and pink curves are those de-noised further adopting KF and ARMA, respectively. The black line is the theoretical Kolmogorov –5/3 slope.

and have a flat plateau at high frequencies. The shape of the spectrum deviates greatly from the –5/3 slope from approximately 0.8 Hz for the horizontal velocity u owing to the presence of strong noise (Fig. 2a), while it deviates from 4 Hz for the vertical velocity w (Fig. 2b). In this case, the noise level for u is approximately 42 times that for w, which is close to what was found in previous studies (Wolk et al., 2002). The plateau is usually the result of measurement noise (Voulgaris and Trowbridge, 1998) and spectral aliasing due to the finite sampling frequency (Kirchner, 2005).

When applying KF or ARMA, noise is appreciably reduced in the time series of velocities, especially for u (Fig. 1). In the case of KF, the spectrum of the de-noised u well follows the –5/3 slope until 3 Hz (Fig. 2a). In the case of ARMA, the spectrum of the de-noised u is slightly higher than the –5/3 slope at high frequencies, which implies that some noise energy is retained although this method eliminates most of the noise. For w with a relatively low noise level, the flat noise plateau is also successfully removed, and the spectra roll off from the –5/3 slope at higher frequencies when de-noised adopting KF or ARMA (Fig. 2b). Figure 3 presents the de-noising performance of these two methods in Exp A3, showing similar results.

The Reynolds decomposition of the velocity of flow without the effects of surface waves is

$$u = U + u', \quad w = W + w', \tag{9}$$

where U and W are the time-averaged velocity components, and u' and w' are the corresponding velocity fluctuations. U and W are defined as

$$U = \frac{1}{N}\sum_{i=1}^{N} u_i, \quad W = \frac{1}{N}\sum_{i=1}^{N} w_i, \tag{10}$$

where N is the total number of samples in each experiment. The RMS of the velocity is usually used to evaluate the turbulent intensity (Variano and Cowen, 2008), which is defined as

$$u_{\mathrm{rms}} = \left(\overline{u'^2}\right)^{1/2}, \quad w_{\mathrm{rms}} = \left(\overline{w'^2}\right)^{1/2}. \tag{11}$$

The turbulent kinetic energy (TKE) is then

$$\mathrm{TKE} = (u_{\mathrm{rms}}^2 + v_{\mathrm{rms}}^2 + w_{\mathrm{rms}}^2)/2. \tag{12}$$

The Reynolds stress is a fundamental variable in turbulent flows and is expressed as

$$\tau = -\rho\overline{u'w'}, \tag{13}$$

where ρ is the density of the water.

As expected, the mean flow speeds are almost unchanged after de-noising adopting KF and ARMA because the noise removed is mainly white noise (Fig. 4a), while the horizontal RMS velocities are appreciably lower than those de-spiked only (Figs 4b and c). In Exp A2, u_{rms} is 2.04 cm/s for the de-spiked velocity, but only 1.27 cm/s for the velocity de-noised adopting KF and 1.30 cm/s for the velocity de-noised adopting ARMA. Correspondingly, the TKE also decreases (Fig. 5a). In Exp A2, the TKE is approximately 3.60×10^{-4} m^2/s^2 for the original velocities, while it is 1.76×10^{-4} m^2/s^2 when adopting KF and 1.78×10^{-4} m^2/s^2 when adopting ARMA; these TKEs are less than half the original TKE. Figure 6 shows accumulative power spectra of u and w in Exp A2. It is seen that the decreases in RMS velocities and then the TKE are mainly due to the attenuation of energy at high frequencies after de-noising adopting both KF and ARMA, especially for the along-stream velocity u (Fig. 6a). Generally, the de-noised u_{rms} and v_{rms} are respectively around 22%–59% and 29%–68% lower than the original values, and the TKE reduces by around 36%–82% in these experiments. Compared with changes in u_{rms} and v_{rms}, the de-noised w_{rms} changes little (Fig. 4d). This is because the noise level of the vertical velocity is relatively low (Figs 2b and 3b).

The Doppler noise in three-dimensional ADV velocities is not independent, and the Reynolds stress is potentially affected by this noise (Nikora and Goring, 1998). However, some previous studies argued that the effect of Doppler noise on Reynolds stress

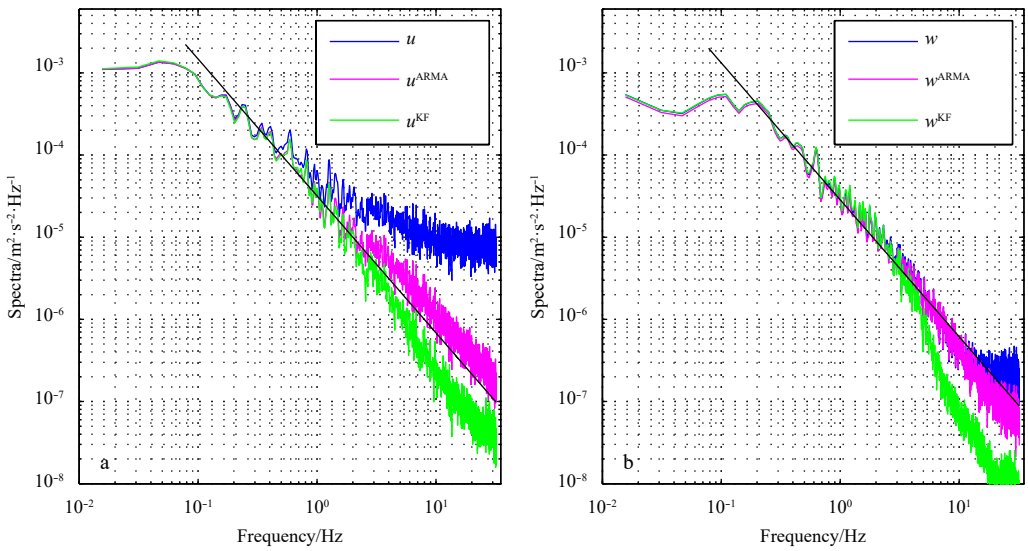

Fig. 3. Power spectra of along-stream (a) and vertical velocities (b) in Exp A3. Blue curves are the power spectra of de-spiked velocities while green and pink curves are those de-noised further adopting KF and ARMA, respectively. The black line is the theoretical Kolmogorov –5/3 slope.

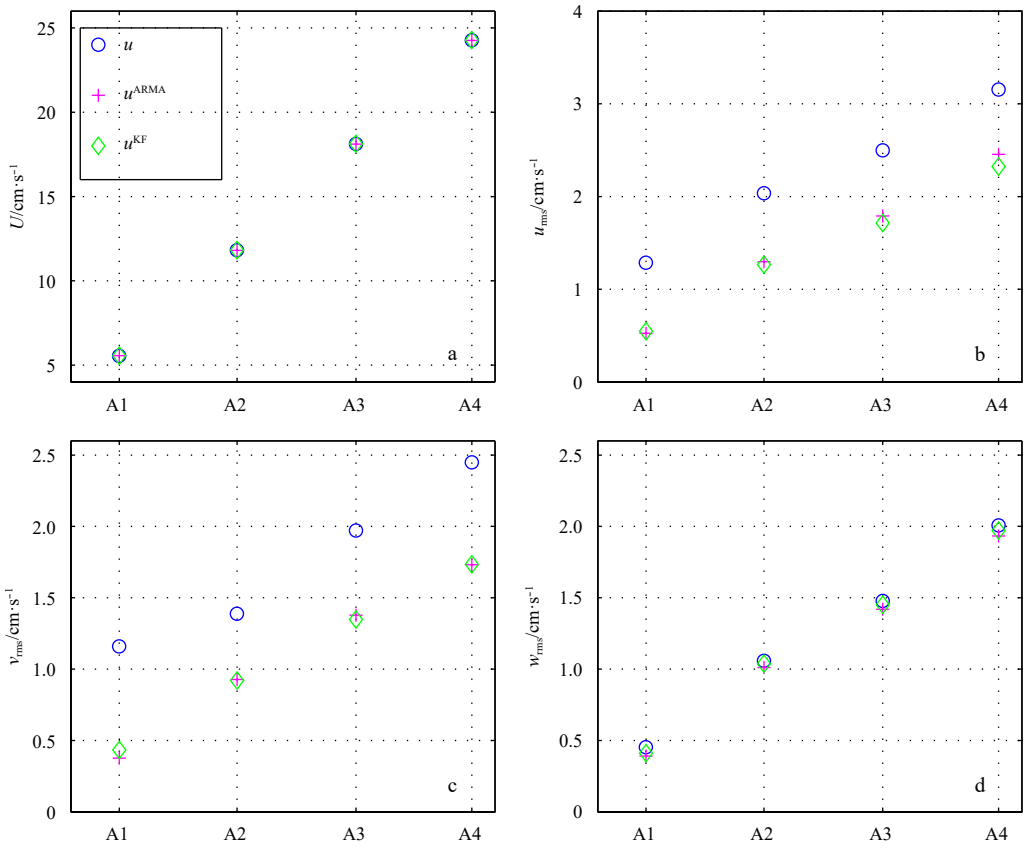

Fig. 4. Time-averaged along-stream velocities (a), along-stream (b), cross-stream (c), vertical RMS velocities (d) in four laboratory experiments. Blue circles are the results for de-spiked velocities while green diamonds and pink crosses are those de-noised further adopting KF and ARMA, respectively.

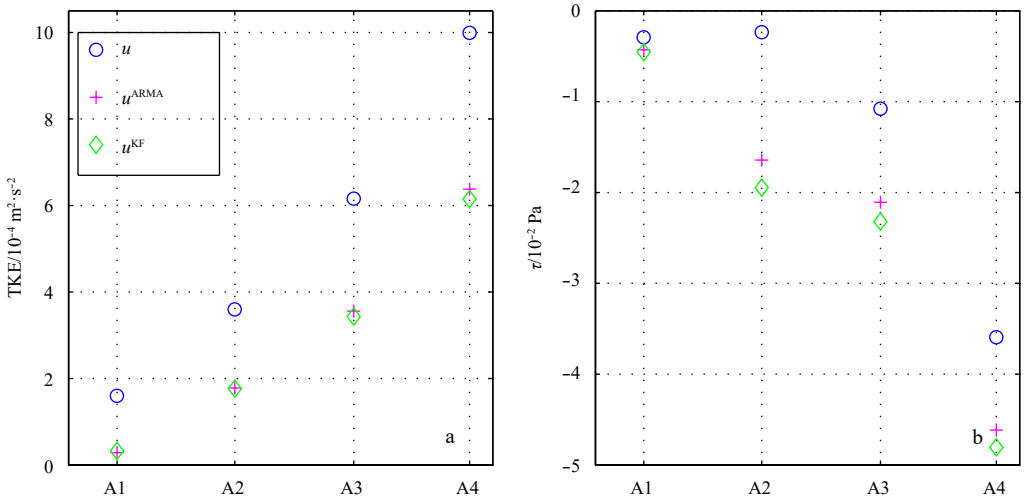

Fig. 5. TKE (a) and the Reynolds stress (b) estimated in four laboratory experiments. Blue circles are the results for de-spiked velocities while green diamonds and pink crosses are those de-noised further adopting KF and ARMA, respectively.

is negligible (Bian et al., 2018) or very small (McLelland and Nicholas, 2000). As an example, Voulgaris and Trowbridge (1998) found that Reynolds stress measured by an ADV was underestimated by only 1% in their experiments. This is not the case for our experiments with high noise levels. In our experiments, Reynolds stress changed appreciably when de-noised adopting KF and ARMA (Fig. 5b). This change is largely due to the decrease in cospectral energy at high frequencies (Fig. 7). Strong Doppler noise thus affects computations of Reynolds stress, and the process of de-noising can reduce uncertainty in these calculations.

4 Offshore observation

A burst was selected to estimate the de-noising performance of KF and ARMA in oceanic measurements. This burst was meas-

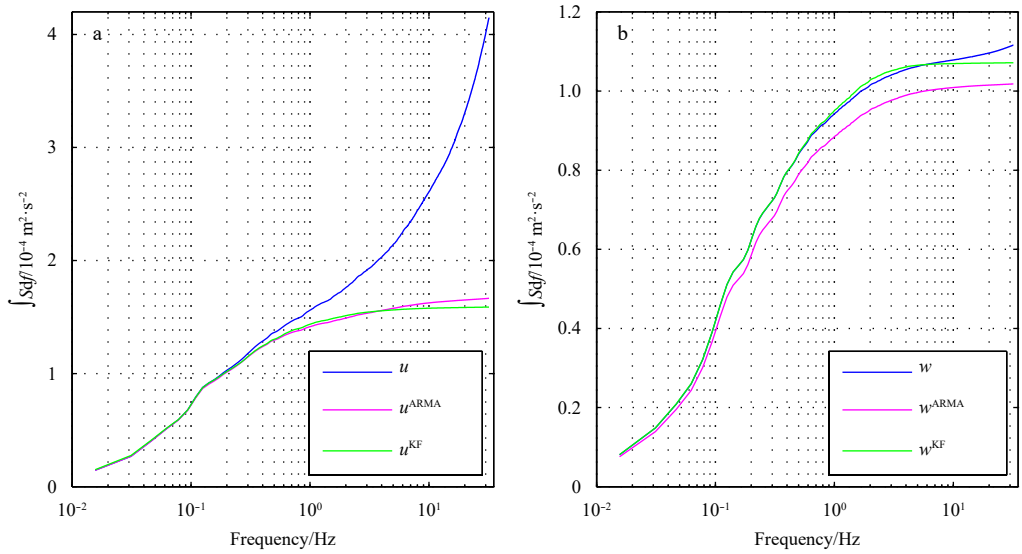

Fig. 6. Accumulative power spectra of along-stream (a) and vertical velocities (b) in Exp A2. Blue curves are the accumulative power spectra of de-spiked velocities while green and pink curves are those de-noised further adopting KF and ARMA, respectively.

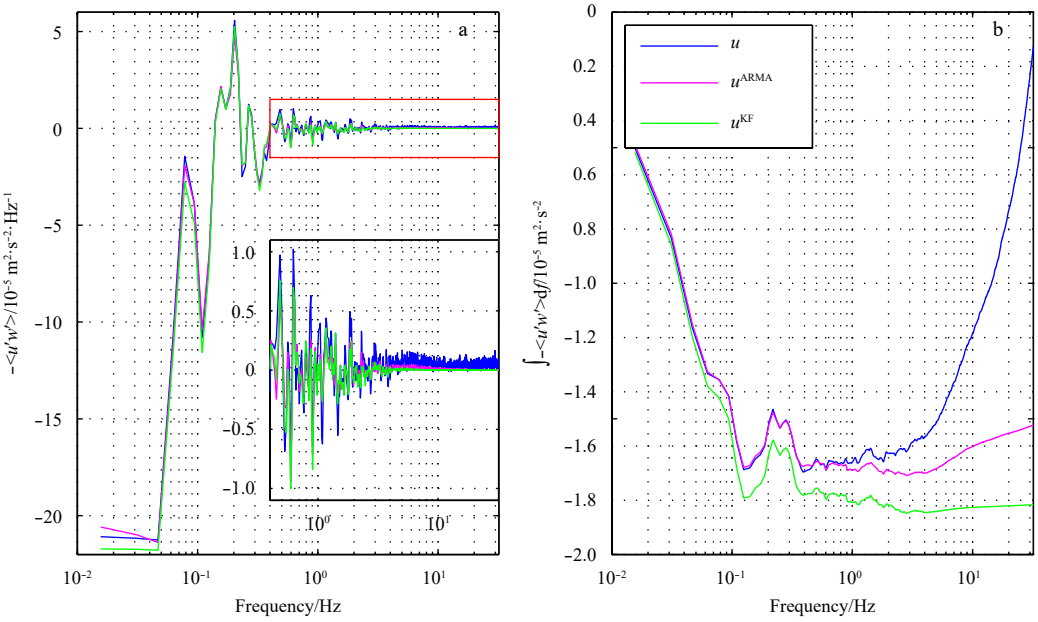

Fig. 7. Cospectra (a) and accumulative cospectra (b) of along-stream and vertical velocity fluctuations in Exp A2. Blue curves are cospectra and accumulative cospectra of de-spiked velocities while green and pink curves are those de-noised further adopting KF and ARMA, respectively.

ured near an observation platform of marine meteorology tower off the northern coast of the South China Sea (Huang et al., 2018). This platform has a water depth of approximately 16 m. This ADV was fixed to a bottom-mounted frame, and the sampling volume was located 0.88 m above the floor. The sampling frequency was set to a rate of 64 Hz, and the velocity range was set to 1 m/s to fit the tide currents and the orbital velocity of surface waves. The sampling time was set to 180 s for every period of 30 min, and then there were 11 520 samples for this burst.

The time series of velocities measured in this burst is shown in Fig. 8, while the power spectra are shown in Fig. 9. In coastal waters, measured velocities are affected by surface waves, and the effects of surface waves are usually superimposed on intermediate frequency bands of velocity spectra. For the de-spiked u, the spectrum has an obvious peak at a frequency around 0.1 Hz. This is in good agreement with the –5/3 slope in log-log space at frequencies from 0.4 Hz to 1.0 Hz. At higher frequencies, there is an obvious noise floor.

Although the flow velocities in this burst are strongly affected by surface waves, the noise is still appreciably reduced by de-noising adopting KF or ARMA (Fig. 8). In the case of the de-noised spectrum, the noise floor is removed and the inertial subrange has a longer available spectrum band, while the low-frequency domain is almost unchanged (Fig. 9a). The vertical velocity has a relatively low noise floor. Additionally, the flat noise plateau at high frequencies is eliminated using the two methods (Fig. 9b).

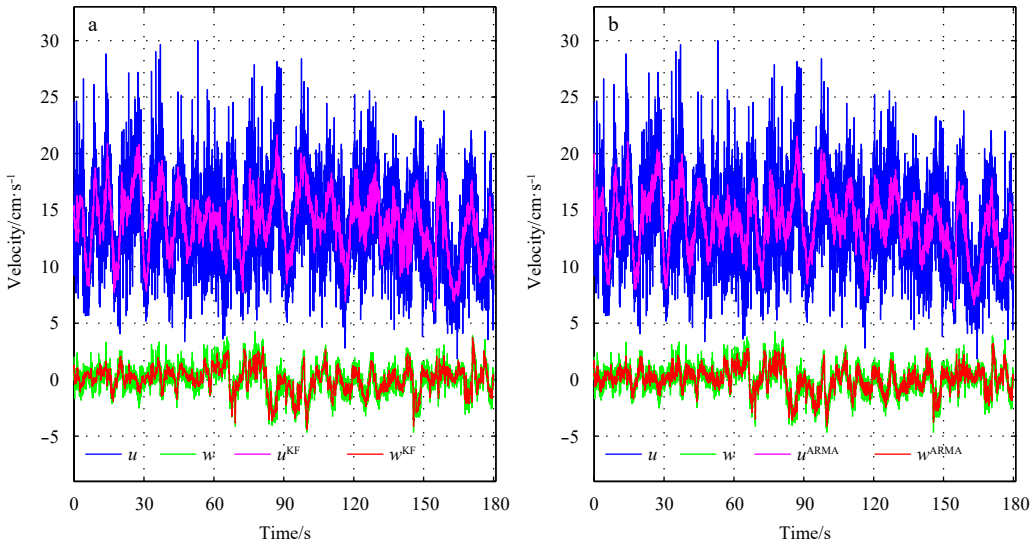

Fig. 8. Time series of de-spiked and de-noised velocities for a burst in offshore observations: KF (a) and ARMA (b). Blue and green curves are de-spiked along-stream and vertical ADV velocities, while pink and red curves are respectively those further de-noised.

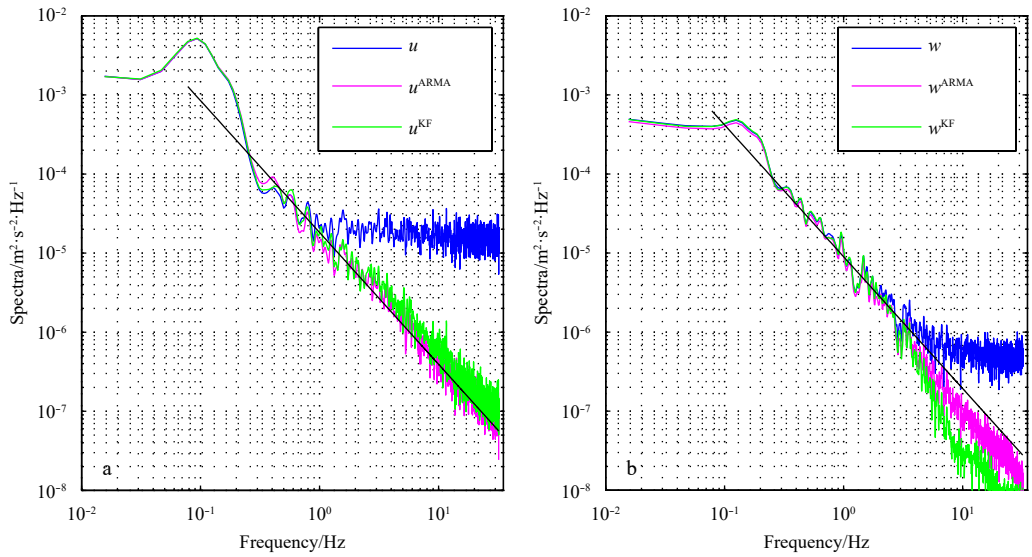

Fig. 9. Power spectra of along-stream (a) and vertical velocities (b) for a burst in offshore observations. Blue curves are the power spectra of de-spiked velocities while green and pink curves are those de-noised further adopting KF and ARMA, respectively. The black line is the theoretical Kolmogorov –5/3 slope.

5 Conclusions

The ADV is a crucial instrument for measurements of oceanic turbulence at fixed points. However, its high-frequency measurements of velocity suffer from a high level of noise, which affects estimates of turbulence statistics. Both laboratory experiments and offshore observations were conducted to evaluate the performance of two commonly used de-noising methods, namely the adoption of KF and ARMA, in terms of eliminating noise in ADV turbulent measurements. A typical three-receiver ADV with a relatively wide velocity range and high sampling frequency was used in these experiments, and the measured velocities were found to much high noise energy levels, especially in their horizontal components.

The results show that the two methods potentially reduce the level of noise in ADV velocities and improve the accuracy of turbulence measurements, even under the effects of surface waves. De-noising adopting the two methods effectively removed the noise floor at high frequencies of the velocity spectra, leading to a longer subrange fitting the Kolmogorov –5/3 slope. Values of the mean velocity are almost unchanged, while other turbulence statistics, such as the RMS horizontal velocities and thus the TKE, decrease appreciably. The results also show that the Reynolds stress estimated from the ADV datasets are affected by Doppler noise in cases with high noise levels, and de-noising processing can thus reduce uncertainties in estimating the Reynolds stress.

It is finally noted that the present study only examined the abilities of the two methods to eliminate noise in ADV velocity datasets. Further research, including the applicability and optimization of parameters involved, is needed to improve the application of the methods in ADV denoising.

References

Bian Changwei, Liu Zhiyu, Huang Yongxiang, et al. 2018. On estimating turbulent Reynolds stress in wavy aquatic environment. Journal of Geophysical Research: Oceans, 123(4): 3060–3071, doi: 10.1002/2017JC013230

Bluteau C E, Jones N L, Ivey G N. 2011. Estimating turbulent kinetic energy dissipation using the inertial subrange method in environmental flows. Limnology and Oceanography: Methods, 9(7): 302–321, doi: 10.4319/lom.2011.9.302

Chang Yang, Chen Yining, Li Yan. 2019. Flow modification associated with mangrove trees in a macro-tidal flat, southern China. Acta Oceanologica Sinica, 38(2): 1–10, doi: 10.1007/s13131-018-1163-y

Chanson H, Trevethan M, Koch C. 2007. Discussion of "Turbulence measurements with acoustic Doppler velocimeters" by Carlos M. Garcìa, Mariano I. Cantero, Yarko Niño, and Marcelo H. Garcìa. Journal of Hydraulic Engineering, 133(11): 1283–1286

Dilling S, MacVicar B J. 2017. Cleaning high-frequency velocity profile data with autoregressive moving average (ARMA) models. Flow Measurement and Instrumentation, 54: 68–81, doi: 10.1016/j.flowmeasinst.2016.12.005

Durgesh V, Thomson J, Richmond M C, et al. 2014. Noise correction of turbulent spectra obtained from acoustic doppler velocimeters. Flow Measurement and Instrumentation, 37: 29–41, doi: 10.1016/j.flowmeasinst.2014.03.001

Elgar S, Raubenheimer B, Guza R T. 2005. Quality control of acoustic Doppler velocimeter data in the surfzone. Measurement Science Technology, 16(10): 1889–1893, doi: 10.1088/0957-0233/16/10/002

Fabozzi F J, Focardi S M, Rachev S T, et al. 2014. The Basics of Financial Econometrics: Tools, Concepts, and Asset Management Applications. New Jersey: John Wiley & Sons, Inc, 171–190

Feddersen F. 2010. Quality controlling surf zone acoustic Doppler velocimeter observations to estimate the turbulent dissipation rate. Journal of Atmospheric and Oceanic Technology, 27(12): 2039–2055, doi: 10.1175/2010JTECHO783.1

García C M, Cantero M I, Niño Y, et al. 2005. Turbulence measurements with acoustic Doppler velocimeters. Journal of Hydraulic Engineering, 131(12): 1062–1073, doi: 10.1061/(ASCE)0733-9429(2005)131:12(1062)

Goring D G, Nikora V I. 2002. Despiking acoustic Doppler velocimeter data. Journal of Hydraulic Engineering, 128(1): 117–126, doi: 10.1061/(ASCE)0733-9429(2002)128:1(117)

Huang Chuanjiang, Ma Hongyu, Guo Jingsong, et al. 2018. Calculation of turbulent dissipation rate with acoustic Doppler velocimeter. Limnology and Oceanography: Methods, 16(5): 265–272, doi: 10.1002/lom3.10243

Hurther D, Lemmin U. 2001. A correction method for turbulence measurements with a 3D acoustic Doppler velocity profiler. Journal of Atmospheric and Oceanic Technology, 18(3): 446–458, doi: 10.1175/1520-0426(2001)018<0446:ACMFTM>2.0.CO;2

Islam M R, Zhu D Z. 2013. Kernel density-based algorithm for despiking ADV data. Journal of Hydraulic Engineering, 139(7): 785–793, doi: 10.1061/(ASCE)HY.1943-7900.0000734

Kalman R E. 1960. A new approach to linear filtering and prediction problems. Journal of Basic Engineering, 82(1): 35–45, doi: 10.1115/1.3662552

Khorsandi B, Mydlarski L, Gaskin S. 2012. Noise in turbulence measurements using acoustic Doppler velocimetry. Journal of Hydraulic Engineering, 138(10): 829–838, doi: 10.1061/(ASCE)HY.1943-7900.0000589

Kirchner J W. 2005. Aliasing in $1/f^{\alpha}$ noise spectra: Origins, consequences, and remedies. Physical Review E, 71(6): 066110, doi: 10.1103/PhysRevE.71.066110

Lemmin U, Lhermitte R. 1999. ADV measurements of turbulence: Can we improve their interpretation?.. Journal of Hydraulic Engineering, 125(9): 987–988, doi: 10.1061/(ASCE)0733-9429(1999)125:9(987)

McLelland S J, Nicholas A P. 2000. A new method for evaluating errors in high-frequency ADV measurements. Hydrological Processes, 14(2): 351–366, doi: 10.1002/(SICI)1099-1085(20000215)14:2<351::AID-HYP963>3.0.CO;2-K

Moore B. 2012. Kalman Filter Package, Version 1.0.0.0. Implements Kalman filter, extended Kalman filter, dual Kalman filter, and square root Kalman filters. www.mathworks.com/matlabcentral/fileexchange/38302-kalman-filter-package [2012-09-24/2019-09-03]

Mori N, Suzuki T, Kakuno S. 2007. Noise of acoustic Doppler velocimeter data in bubbly flows. Journal of Engineering Mechanics, 133(1): 122–125, doi: 10.1061/(ASCE)0733-9399(2007)133:1(122)

Neusser K. 2016. Time Series Econometrics. Switzerland: Springer International Publishing, 25–44

Nikora V I, Goring D G. 1998. ADV measurements of turbulence: Can we improve their interpretation?.. Journal of Hydraulic Engineering, 124(6): 630–634, doi: 10.1061/(ASCE)0733-9429(1998)124:6(630)

Parsheh M, Sotiropoulos F, Porte-Agel F. 2010. Estimation of power spectra of acoustic-Doppler velocimetry data contaminated with intermittent spikes. Journal of Hydraulic Engineering, 136(6): 368–378, doi: 10.1061/(ASCE)HY.1943-7900.0000202

Pope S B. 2000. Turbulent Flows. Cambridge, UK: Cambridge University Press, 219–242

Qi Yongfeng, Shang Xiaodong, Chen Guiying, et al. 2020. Eddy covariance measurements of turbulent fluxes in the surf zone. Acta Oceanologica Sinica, 39(3): 63–72, doi: 10.1007/s13131-020-1562-8

Qiao Fangli, Yuan Yeli, Deng Jia, et al. 2016. Wave-turbulence interaction-induced vertical mixing and its effects in ocean and climate models. Philosophical Transactions of The Royal Society A: Mathematical, Physical and Engineering Sciences, 374(2065): 20150201, doi: 10.1098/rsta.2015.0201

Saddoughi S G, Veeravalli S V. 1994. Local isotropy in turbulent boundary layers at high Reynolds number. Journal of Fluid Mechanics, 268: 333–372, doi: 10.1017/S0022112094001370

SonTek. 2001. Acoustic Doppler velocimeter principles of operation. SonTek/YSI Technical Notes. San Diego: SonTek, 1–14

Variano E A, Cowen E A. 2008. A random-jet-stirred turbulence tank. Journal of Fluid Mechanics, 604: 1–32, doi: 10.1017/S0022112008000645

Voulgaris G, Trowbridge J H. 1998. Evaluation of the acoustic Doppler velocimeter (ADV) for turbulence measurements. Journal of Atmospheric and Oceanic Technology, 15(1): 272–289, doi: 10.1175/1520-0426(1998)015<0272:EOTADV>2.0.CO;2

Wahl T L. 2003. Discussion of "Despiking acoustic Doppler velocimeter data" by Derek G. Goring and Vladimir I. Nikora. Journal of Hydraulic Engineering, 129(6): 484–487

Welch G, Bishop G. 1995. An introduction to the Kalman filter. Technical report. Chapel Hill, NC, United States: University of North Carolina at Chapel Hill, 1–16

Wolk F, Yamazaki H, Seuront L, et al. 2002. A new free-fall profiler for measuring biophysical microstructure. Journal of Atmospheric and Oceanic Technology, 19(5): 780–793, doi: 10.1175/1520-0426(2002)019<0780:ANFFPF>2.0.CO;2